Epilepsia, **40**(9):1198–1209, 1999
Lippincott Williams & Wilkins, Inc., Philadelphia

Laboratory Research

Mutated Nicotinic Receptors Responsible for Autosomal Dominant Nocturnal Frontal Lobe Epilepsy are More Sensitive to Carbamazepine

F. Picard, S. Bertrand, *O. K. Steinlein, and D. Bertrand

*Department of Physiology, Faculty of Medicine, University of Geneva, Switzerland; and *Institute of Human Genetics, University of Bonn, Bonn, Germany*

Summary: *Purpose:* The recent linkage between a genetically transmissible form of epilepsy (ADNFLE) and mutations within the α_4 subunit, one component of the major brain neuronal nicotinic acetylcholine receptor (nAChR), raises the question of the role of this receptor in epileptogenesis. Although acting by different mechanisms, the two genetic alterations so far identified both render the nAChR less efficient. In view of the high sensitivity of ADNFLE to carbamazepine (CBZ), we studied the effects of this drug and of valproate (VPA) on the human $\alpha_4\beta_2$ nAChR and its mutations.

Methods: The $\alpha_4\beta_2$ nAChRs from control and mutant α_4 subunits were reconstituted in *Xenopus* oocytes and investigated by using a dual-electrode voltage clamp technique. Acetylcholine (ACh)-evoked currents recorded in the absence or presence of antiepileptic drugs (AEDs) were studied to analyze the mode of action of these compounds.

Results: ACh-evoked currents at the human $\alpha_4\beta_2$ nAChR were readily and reversibly inhibited by ~100 μM CBZ. This compound was found to be a noncompetitive inhibitor of the nAChR, which probably acts by entering the channel and causing a blockade by steric hindrance. Dose–response inhibition curves determined on the control receptor and on ADNFLE-mutant receptors showed a greater sensitivity of the mutants to CBZ, with median inhibitory concentrations (IC_{50}s) in the range of the antiepileptic plasma levels of CBZ. In contrast, VPA had nearly no effect on control and mutant nAChRs.

Conclusions: CBZ inhibits the neuronal $\alpha_4\beta_2$ nAChRs at pharmacologic concentrations, with ADNFLE mutants displaying about threefold higher sensitivity to this compound. The increased sensitivity of these mutant receptors supports the hypothesis that the antiepileptic activity of CBZ can, at least to some extent, be attributed to the nAChR inhibition. **Key Words:** Nicotinic acetylcholine receptor—Antiepileptic—Carbamazepine—Physiology—ADNFLE.

Most efficacious antiepileptic drugs (AEDs) used in the treatment of patients with partial epilepsies include carbamazepine (CBZ), phenytoin (PHT), valproate (VPA), phenobarbital (PB), and more recently, oxcarbazepine (OCBZ), lamotrigine (LTG), and vigabatrin (VGB). This list is far from exhaustive, and the rank of potency of these drugs largely depends on the epilepsy underlying pathophysiologic mechanisms. The mechanisms of action of most AEDs still remain speculative.

Electrophysiologic investigations revealed that CBZ acts on several membrane proteins including voltage-dependent sodium or calcium channels (1–5) as well as on ligand-gated channels such as *N*-methyl-D-aspartate (NMDA), γ-aminobutyric acid (GABA), or nicotinic acetylcholine receptors (nAChRs) in chromaffin cells (6–8). Although many of these effects may occur at concentrations higher than those found in the plasma (20–50 μM) and cerebrospinal fluid [typically 20–30% of the plasma level (9)] of patients with epilepsy they all suggest that CBZ acts directly on integral membrane proteins involved in the signal transmission across neurons or in the regulation of the overall cell excitability.

The recent finding that a form of nocturnal partial epilepsy, the autosomal dominant nocturnal frontal lobe epilepsy (ADNFLE), is linked to a missense or insertion mutation in the gene coding for the neuronal nAChR α_4 subunit (10,11) indicates that a misfunctioning of these ligand-gated receptors may play a role in triggering synchronous discharges responsible for epilepsy. The effect of both genetic alterations presently known is to reduce nAChR function (11–13); however, the ADNFLE patho-

Accepted February 11, 1999.
Address correspondence and reprint requests to Dr. D. Bertrand at Department of Physiology, C.M.U., 1, rue Michel Servet, CH-1211 Geneva 4, Switzerland. E-mail: Bertrand@ibm.unige.ch

genesis from electrophysiologic alterations to clinical phenotype remains to be elucidated.

The observation that ADNFLE is best treated by CBZ (14–16) prompted us to examine the action of this compound on the α_4-containing human neuronal nAChR. The action of VPA, generally not effective in controlling ADNFLE seizures (14), also was analyzed for comparison. Electrophysiologic and pharmacologic investigations were conducted on human $\alpha_4\beta_2$ ($h\alpha_4\beta_2$) neuronal nAChR reconstituted in *Xenopus* oocytes either with the control α_4 subunit or with the two mutant forms presently characterized in ADNFLE.

METHODS

cDNAs and mutagenesis

The neuronal α_4 and β_2 subunits have been cloned as previously described into the pSPoD expression vector (12). The mutations found in ADNFLE patients were introduced into the α_4 cDNA. For this purpose, part of the exon 5 was amplified by polymerase chain reaction (PCR) from patients' DNA by using the following primers: ACCTGACCAAGGCCCACCTG and GCTCGGGCCAGAAGCGCGG for S248F; and CCTGCCCTCCGAGTGTGGC and GCTCGGGCCAGAAGCGCGG for 776ins3. The amplified DNA fragments were then transferred into the α_4 subunit by using *Dra*III/*Mun*I restriction sites both for the 776ins3 and for the S248F mutation. Plasmids with the S248F mutant allele were identified by a PCR assay with one of the primers creating a new *Hpa*II restriction site only in the wild-type allele (10). The subclones carrying the 776ins3 allele were identified by SSCA (single-strand conformation analysis). The presence of both mutations was further confirmed by sequencing.

Oocyte preparation, cDNA injection

Oocytes were prepared according to the standard procedure (17) and nuclear-injected with 10 nl of buffer containing equal concentrations (0.1 μg/μl) of α and β subunit cDNAs. Cells were kept at 18°C in BARTH medium for 2–3 days before the electrophysiologic investigation. To improve cell survival and minimize possible contamination, each oocyte was placed in a separate well of an 8 × 12 microtiter plate (NUNC).

Drugs and solutions

BARTH medium was made as follows: 88 m*M* NaCl, 1 m*M* KCl, 2.4 m*M* $NaHCO_3$, 10 m*M* HEPES, 0.82 m*M* $MgSO_4 \cdot 7\ H_2O$, 0.33 m*M* $Ca(NO_3)_2 \cdot 4\ H_2O$, 0.41 m*M* $CaCl_2 \cdot 6\ H_2O$, pH 7.4 adjusted with NaOH, and supplemented with antibiotics (kanamycin, 20 μg/ml; penicillin, 100 μ/ml; and streptomycin, 100 μg/ml). To prevent bacterial and fungal contaminations, this solution was filtered with a 0.2-μm filter and kept sterile. The control medium contained 82.5 m*M* NaCl, 2.5 m*M* KCl, 5 m*M* HEPES, 2.5 m*M* $BaCl_2$, 1 m*M* $MgCl_2$, pH 7.4 adjusted with NaOH. ACh was prepared as stock solution at 0.1 *M* and stored at −20°C. CBZ and VPA were dissolved in 100% ethanol and water, respectively, and diluted at final concentrations in control medium immediately before the experiment. All drugs and chemicals were obtained from either Fluka, Sigma, or Research Biochemicals International (RBI) (Buchs, Switzerland).

Electrophysiologic recording and data analysis

Recordings were made by using the two-electrode voltage clamp technique. Electrodes pulled from borosilicate glass were filled with 3 *M* KCl. Voltage clamp was done by using a GENECLAMP amplifier (Axon Instruments, Foster City, CA, U.S.A.). Data were captured on-line on a personal computer (PC) equipped with an analog-to-digital converter (AT-MIO16D from National Instrument, Austin, TX, U.S.A.). During the experiments, oocytes were continuously superfused with control solution, and drugs were applied by using a fast-switching solution system made with computer-controlled electrovalves (type 3, General Valve). To equilibrate the AED concentration, cells were usually preincubated for 20 s with the AED before being exposed to ACh. For the dose–response inhibitions, ACh concentrations and duration of application depended on the type of receptor studied (control, S248F-, or 776ins3-containing receptor) because of differences in median effective concentrations (EC_{50}s) and time course profiles.

Dose–response inhibition profile induced by various AED concentrations were adjusted to the empiric Hill equation:

$$y = \frac{1}{1 + \left(\frac{x}{IC_{50}}\right)^{n_H}} \quad (1)$$

where y is the fraction of remaining current, IC_{50} is the concentration of blocking agent causing a 50% reduction of the current evoked by a pulse of agonist near the EC_{50}, n_H is the Hill coefficient, and x is the agonist concentration.

Dose–response relations were adjusted to the empirical Hill equation:

$$y = \frac{1}{1 + \left(\frac{EC_{50}}{x}\right)^{n_H}} \quad (2)$$

where y is the fraction of activated current, EC_{50} is the concentration of agonist evoking a current of half-maximal amplitude, n_H is the Hill coefficient, and x is the agonist concentration.

Voltage-ramp protocols were performed as follows: the membrane was held at 40 mV, and a first ramp (from

+ 40 to −100 mV in 2 s) was applied in the standard saline medium (without agonist) for the determination of the leak current. About 1 min later, 16 μ*M* ACh was delivered for 30 s, and the voltage-ramp was applied 10 s after the onset of the drug delivery. Data presented herein were subtracted from the leak current. The conductance was calculated with the following equation:

$$g = i / (v - E_{rev}) \quad (3)$$

where g is the conductance [nS], i is the current [nA], v is the holding voltage [mV], and E_{rev} is the reversal potential for $\alpha_4\beta_2$ that is ~−7 mV (18).

All values are given with their respective standard deviations (SD). Unless indicated, cells were held throughout the experiments at −100 mV.

Data analyses were carried off-line on a Macintosh computer (Apple, type 8500/150) by using a home-made program. Curves were adjusted by using a least-square minimization procedure (SIMPLEX).

RESULTS

ACh-evoked currents at the h$\alpha_4\beta_2$ nAChRs are readily and reversibly inhibited by a 100 μ*M* concentration of CBZ. In these experiments, a steady-state concentration of CBZ was obtained by first incubating the receptor in a determined concentration of the drug for 20 s and then coapplying it with the natural agonist ACh (3 μ*M;* Fig. 1A). Typical ACh-evoked currents recorded with this protocol for three CBZ concentrations are shown in the

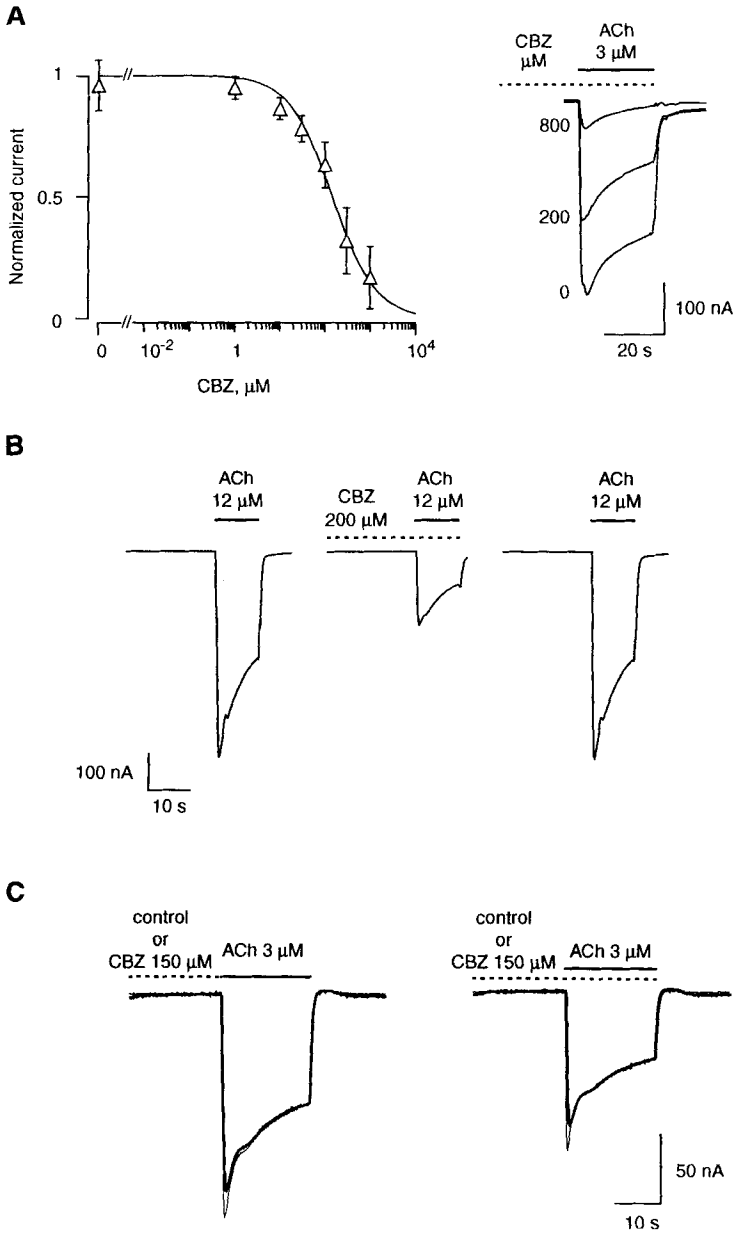

FIG. 1. Carbamazepine (CBZ) inhibits the neuronal nicotinic acetylcholine receptor (nAChR) at clinically relevant concentrations. **A:** ACh-evoked currents are inhibited in a dose-dependent manner by CBZ. **Left:** Dose–response inhibition measured at the plateau and plotted as a function of the logarithm of CBZ concentration. Currents were evoked by 3 μ*M* ACh. Line through data points corresponds to the best fit obtained with the empiric Hill equation (Eq. 1) with an IC_{50} of 140.5 ± 85 μ*M* and n_H of 0.85 ± 0.09 (n = 9 cells). Typical currents recorded in three CBZ concentrations are shown in the **right panel.** Dashed line, the time of CBZ application; continuous line, the time of ACh application. **B:** CBZ inhibition is fully reversible. Responses recorded in the same cell before, during CBZ, and after 2-min washout are illustrated. **C:** Preapplication of CBZ caused no significant reduction of the subsequent ACh-evoked current (thick trace, **left panel**). The control response recorded before any manipulation is represented by the thin trace. Application of the same CBZ concentration, in the same cell, together with ACh led to an important reduction of the current (thin trace, **right panel**). Pre- and coapplication, which established a steady concentration of CBZ, resulted in no further reduction of the response (thick trace, **right panel**).

right panel of Fig. 1A. Measurement of the peak and plateau of the ACh-evoked currents recorded in these conditions yielded a dose–response inhibition profile that was adequately fitted by the empirical Hill equation (Eq. 1). A mean half inhibition (IC_{50}) of 140.5 ± 85 μM (n_H = 0.85 ± 0.09) was determined for the plateau response, and 165 ± 101 μM (n_H = 0.85 ± 0.09) for the peak response (data not represented). These values are above the known AED plasma levels of CBZ (20–50 μM). As shown in Fig. 1B, CBZ effects are fully reversible within 2 min, indicating that this compound does not strongly bind to the receptor. Experiments designed to determine the recovery time course from CBZ blockade revealed that unbinding of CBZ was not affected significantly by the presence or absence of the agonist (data not shown). To assess through which state CBZ interacts with the nAChR, pre- and coapplication experiments were designed. As shown in Fig. 1C (thick trace, left panel) preapplication of CBZ caused no modification of the holding current or significant alteration of the subsequent ACh-evoked current. In contrast, when the same concentration of CBZ was applied on the same cell but concomitant with the agonist, a marked reduction of the response was observed (thin trace, right panel). Thus, to better analyze CBZ effects, all further experiments were carried out with both a pre- and coapplication that allows establishment of a steady-state concentration of the antagonist. Because CBZ was diluted in ethanol (0.4% at 200 μM CBZ), experiments in which the receptor was exposed to the vehicle alone were performed. In agreement with previous findings, no reduction of the ACh-evoked current was observed even for the highest concentration of ethanol used (data not shown). These data indicate that blockade observed during CBZ coapplication is attributable to this compound and not to an indirect effect of the solvent.

Regarding the mode of action of CBZ blockade, distinction between competitive and noncompetitive blockade can be determined on the basis of the following experiments: competitive blockers are identifiable from the fact that inhibition can be overcome by an increase of the agonist concentration. Noncompetitive blockers are compounds that do not interact with the agonist binding site and are characterized by a reduction of the agonist-evoked response that cannot be restored by an increase of the agonist concentration. As a correlate, in noncompetitive blockade, the dose–response curve displays no major shift in the EC_{50}. As shown in the left panel of Fig. 2A, incubation in a fixed CBZ concentration yielded an overall reduction of the agonist dose–response relation without detectable shift in the EC_{50} (16.1 μM ACh, in absence and in presence of CBZ). This is further illustrated by the fact that both curves are readily fitted by the empirical Hill equation (Eq. 2) with identical parameters provided that a scaling factor of 58% is used for all values obtained in presence of CBZ. In the right panel of Fig. 2A, typical currents evoked by several concentrations of ACh are shown in control condition (left side) and in presence of 200 μM CBZ. These curves confirm that the reduction of the current amplitude is independent of ACh concentration, 200 μM CBZ reducing the current to ~58% of its initial value independent of the ACh concentration. Taken together, these data suggest that CBZ acts as a noncompetitive blocker at the $h\alpha_4\beta_2$ nAChR. Noncompetitive blockers mediate their action either by steric hindrance in the ionic pore or by an allosteric modulation of the receptor. In the case of steric hindrance blockade, the compounds are often referred to as open channel blockers (OCBs) because the receptor should be stabilized by the presence of agonist in its open conformation before allowing the compound to enter the channel and act as a sort of molecular cork.

To evaluate the mode of action of CBZ, further, current–voltage (I-V) relations were measured first in control solution and then in presence of this compound (Fig. 2B). These measurements revealed that although the $h\alpha_4\beta_2$ response showed an endogenous nonlinearity with a strong inward rectification, its I-V curve was not significantly affected by the addition of CBZ. Computation of the whole-cell nAChR conductance (Eq. 3), assuming a reversal potential of –7 mV (18), further illustrates the voltage independence of CBZ blockade (Fig. 2C). Although voltage dependence is often used as an OCB landmark, the lack of sensitivity to voltage also can result from the absence of charge on the considered compound, as is the case for CBZ, in which carbamoyl side chain is part of a nonionized urea moiety (19). Moreover, as shown previously on muscle nAChR, distinction between an OCB mode of action and other noncompetitive mechanisms might also be made on the basis of analysis of the response time course (20). ACh-evoked currents recorded in presence of an OCB must show an increased apparent desensitization attributable to the progressive blockade of the channels. Analysis of the ACh-evoked currents in $h\alpha_4\beta_2$-expressing oocytes recorded in control solution or different CBZ concentrations at fixed potential revealed a modification of the response time course with an acceleration of the apparent desensitization in function of the CBZ concentration (Fig. 2D). Altogether these results suggest that CBZ enters the ionic pore of the nAChR.

Because patients with ADNFLE are more sensitive to CBZ than are those with other focal epilepsies (14), we assessed the sensitivity to CBZ of the $\alpha_4\beta_2$ receptor containing the corresponding α_4 mutants S248F or 776ins3. The basal electrophysiologic properties of these mutant receptors had been characterized by reconstitution experiments performed in *Xenopus* oocytes (11–13,21,22). The mutation S248F causes a decrease in the apparent

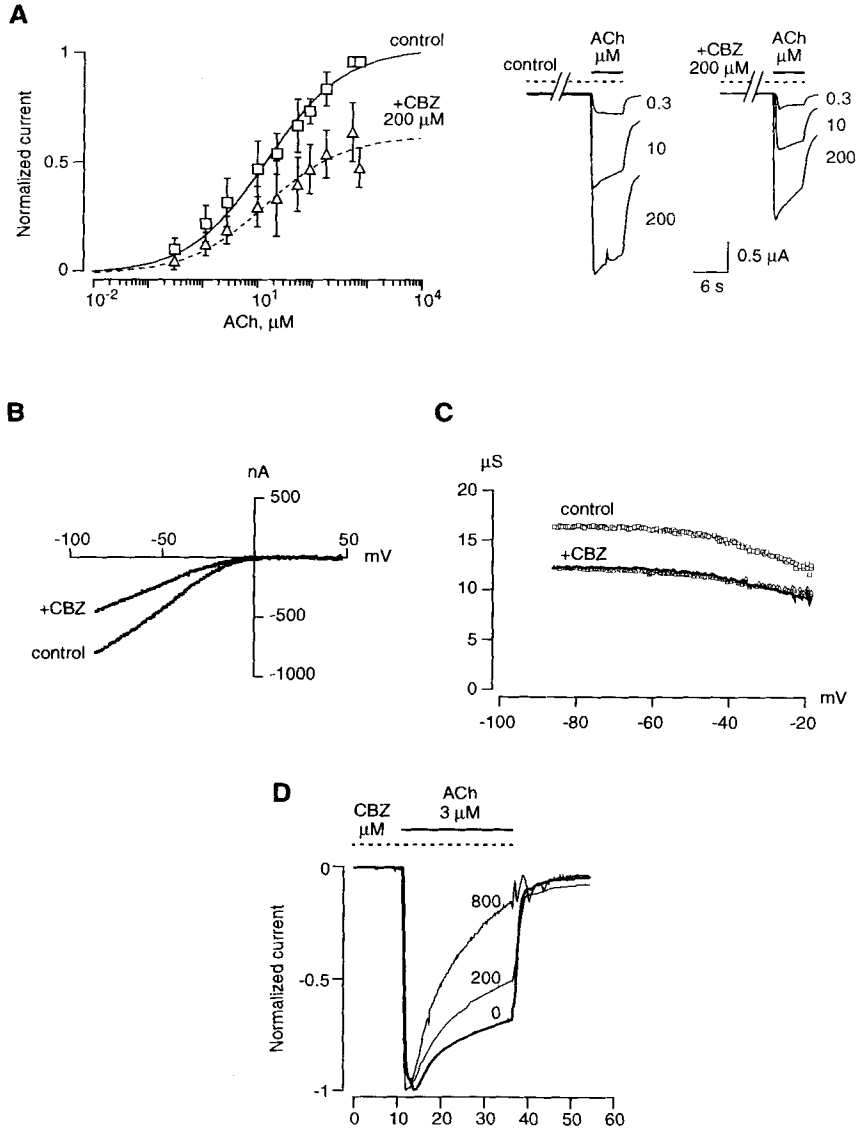

FIG. 2. Carbamazepine (CBZ) is a noncompetitive inhibitor of $h\alpha_4\beta_2$ nicotinic acetylcholine receptor (nAChR). **A:** Mean ACh dose–response curves determined in control (squares) and during a steady exposure to CBZ (triangles) are shown in the **left panel** (n = 7 cells). Continuous line through data points corresponds to Hill equation (Eq. 2) with an EC_{50} of 16.1 ± 7.3 μ*M* and n_H of 0.62 ± 0.04 (control conditions). Data recorded in the same cells in presence of CBZ can be fitted with the identical parameters, providing a scaling factor of 0.58 (dashed line). **Right:** typical currents evoked by three ACh concentrations in absence or in presence of CBZ are superimposed. **B:** CBZ blockade is voltage independent. I–V (current–voltage) relations measured in control (16 μ*M* ACh) and in presence of 100 μ*M* CBZ by using a sawtooth command voltage from +40 to −100 mV. **C:** Conductances derived from data presented in **B** by using Ohm's law (Eq. 3), and assuming a reversal potential at −7 mV, are presented for one cell. Data recorded in presence of CBZ correspond to the control conductance multiplied by a scaling factor of 0.75. Scaling factors determined in two other cells were 0.63 and 0.83, respectively (data not shown; mean, 0.74 ± 0.1). **D:** CBZ accelerates apparent desensitization. Currents corresponding to data shown in **A** were normalized at their peak values and superimposed for comparison. Dashed line, timing of CBZ application.

affinity to ACh, a reduction of the ACh-evoked current measured at saturation, a significant increase in the receptor desensitization (12,22), and a lower permeability to calcium (13). The leucine insertion (776ins3) induces no change in the amplitude of the ACh-evoked current at saturation or in the time course of the response, and even increases the apparent affinity to ACh of the receptor. However, some experiments indicated that it significantly reduces permeability to calcium (11).

Exposure of the S248F containing nAChR to CBZ resulted in a strong dose-dependent inhibition of the ACh-evoked current, as shown in Fig. 3A. Dose–response relations of the peak and plateau currents, measured as previously, yielded in average an IC_{50} of 175 μ*M* for the peak current, whereas half inhibition of the plateau response was observed at 51 μ*M*. When the same experiments were repeated on oocytes expressing the 776ins3 mutant, an even higher sensitivity to CBZ was observed, with the IC_{50} values of peak and plateau of 66.5 and 42 μ*M*, respectively (Fig. 3B). At concentrations of CBZ >50 μ*M*, a small rebound was consistently observed at the end of the application. Further increase in the CBZ concentration yielded a concomitant increase of this rebound (right panel of Fig. 3B). The presence of such rebound in every cell tested with a high CBZ concentration and its absence in any other test indicates that it cannot be attributed to a perfusion artifact but must arise from the CBZ blockade.

As shown in Fig. 3C, measurements of the ACh dose–response curves in control solution and in presence of a fixed CBZ concentration (50 μ*M*) in the 776ins3 mutant showed, as for the $h\alpha_4\beta_2$, an overall reduction of the current amplitude but no shift of the EC_{50} for ACh. To further assess the mode of action of CBZ on the two mutants, ACh-evoked currents recorded in control solution and in presence of CBZ were normalized (Fig. 3D).

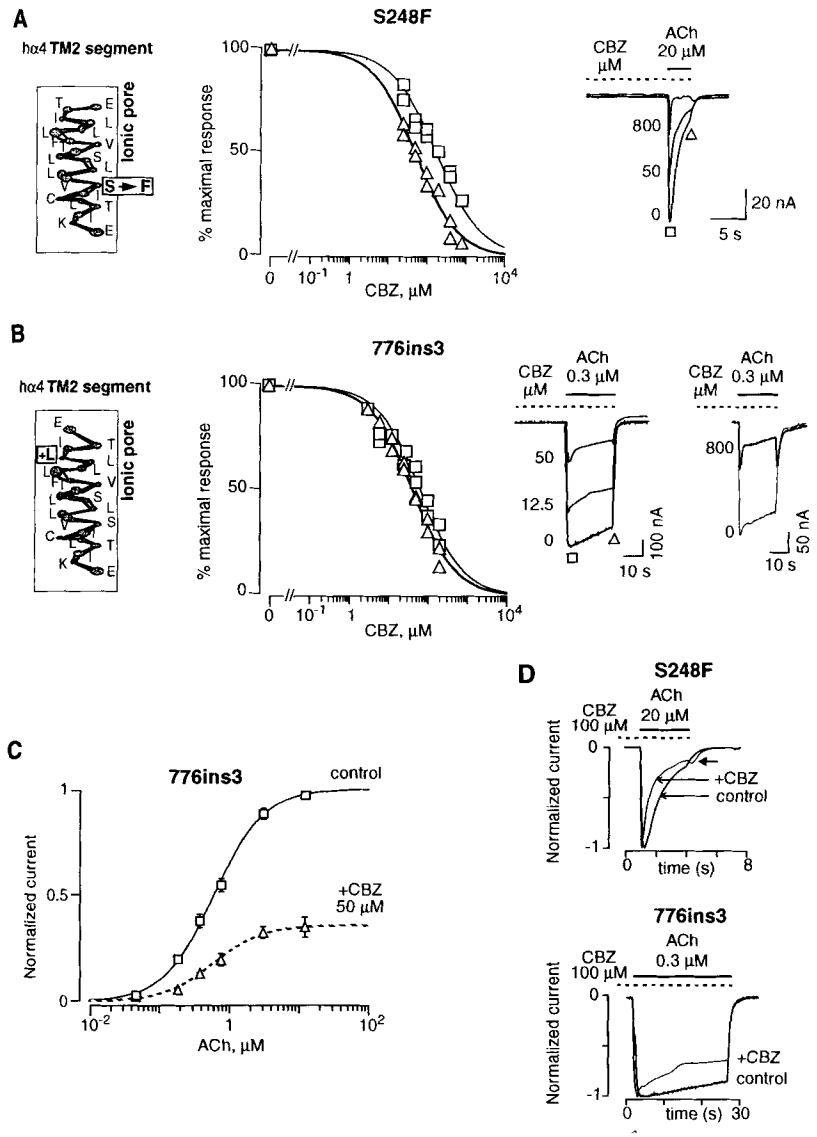

FIG. 3. Differential sensitivity of autosomal dominant nocturnal frontal lobe epilepsy (ADNFLE) mutants to carbamazepine (CBZ). **A:** Schematic representation of the α-helix corresponding to TM2 and the S248F mutation is illustrated on the left. Dose–response inhibition curves of $h\alpha_4(S248F)\beta_2$ nicotinic acetylcholine receptor (nAChR) were measured at peak (squares) or at the plateau current (triangles) (n = 2 cells). Plot of peak and plateau values as a function of the logarithm of CBZ concentration yielded typical dose–response inhibition curves. Lines through data points were computed with the Hill equation (Eq. 1) by using an IC_{50} of 175 μ*M* and n_H of 0.75 for the peak, and 51 μ*M* and 0.8 for the plateau. To minimize desensitization artifact, responses were tested at prolonged intervals (2–4 min). Effects of pre- and coapplications of CBZ at three concentrations on the ACh-evoked currents are shown on the **right.** The ACh concentration used (20 μ*M*) was near the EC_{50} obtained for $h\alpha_4(S248F)\beta_2$ nAChR. **B:** TM2 776ins3 insertion is represented on the **left.** For the dose–response inhibition of $h\alpha_4(776ins3)\beta_2$ nAChR, measurements and computations were done as in **A** (*n* = 2 cells). IC_{50} values of peak and plateau are of 66.5 μ*M* (n_H = 0.8) and 42 μ*M* (n_H = 0.8), respectively. Effects of pre- and coapplications of CBZ at three concentrations on the ACh-evoked currents are shown on the right. A small rebound was consistently observed for all the CBZ concentrations >50 μ*M*. **Extreme right:** A typical rebound observed at the end of a 800 μ*M* CBZ exposure. The ACh concentration used (0.3 μ*M*) was near the EC_{50} obtained for $h\alpha_4(776ins3)\beta_2$ nAChR. **C:** Noncompetitive blockade of $h\alpha_4(776ins3)\beta_2$ nAChR is shown, as it had been for $h\alpha_4\beta_2$ (Fig. 2A). ACh dose–response relation is fitted with the Hill equation (Eq. 2) by using an EC_{50} of 0.61 ± 0.1 μ*M* and n_H of 1.23 ± 0.06 (n = 3 cells, continuous line). Dashed line (CBZ, 50 μ*M*) corresponds to the same values scaled down to 37%. **D:** Normalized ACh-evoked currents recorded in control condition and in presence of 100 μ*M* CBZ are superimposed. **Upper panel:** S248F. Currents obtained for 776ins3 are shown in the **lower panel.**

We can assume that CBZ blocks the S248F channels when they are stabilized in their open conformation, as indicated by the small rebound (solid arrow) at the offset of the drug application.

Use-dependent experiments were performed on the control and mutant receptors. In this experiment, the cell was exposed to a fixed concentration of the tested drug and challenged at periodic intervals with a brief pulse of agonist that contained the same concentration of the drug. For the open channel blockers, a progressive blockade must be observed every time the channels are activated, and blockade must be independent of the time interval between pulses. If the drug acts by another noncompetitive mechanism, the blockade will occur independent of the test pulses but will depend on the drug-exposure duration. As seen in Fig. 4, CBZ effects are readily comparable to those caused by MK-801, which was shown to act as an OCB at the $h\alpha_4\beta_2$ nAChR (23). The evoked current progressively decrease in function of the test pulses independent of the prolonged CBZ interval exposures (150 s). Comparison of the data obtained with the control and the mutant receptors further highlights the increase in apparent affinity of these receptors to CBZ. As expected for a mutation occurring in the channel domain, a reduction in the IC_{50} to MK-801 also was observed for the two mutants (fourfold, data not shown).

To compare the sensitivity of $h\alpha_4\beta_2$ nAChR with that of another common AED, we conducted experiments with VPA. To characterize the possible effects caused by VPA, this compound was pre- and/or coapplied with ACh. Because few or no effects were observed even for concentrations as high as 6.4 m*M* on either $h\alpha_4\beta_2$ or the $h\alpha_4(776ins3)\beta_2$ mutant (Fig. 5), it can be

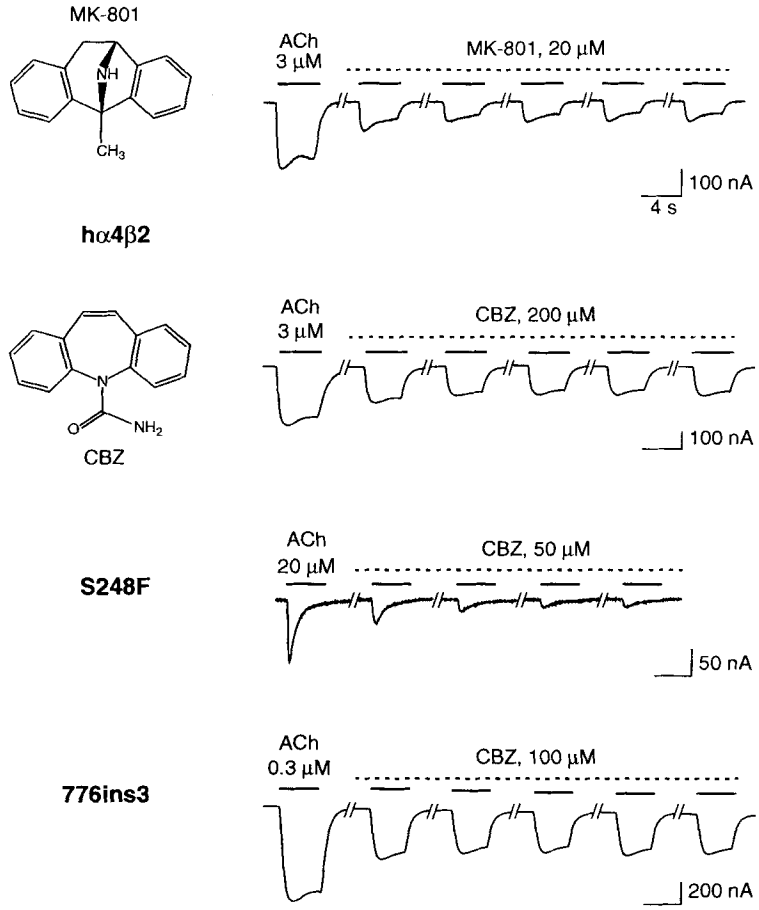

FIG. 4. Use dependence of carbamazepine (CBZ) blockade. Exposure to open channel blockers caused a progressive reduction of the acetylcholine (ACh) evoked test pulses. **Top:** Effects caused by a long exposure to MK-801 on brief ACh responses (3 μ*M*, 4 s). Responses were tested once every 150 s. **Left:** Chemical structure of this tricyclic agent. When the same experiment was repeated in presence of CBZ (200 μ*M*), a progressive reduction of the ACh-evoked responses was observed. CBZ chemical structure on the **left. Bottom:** Effects of CBZ on a S248F- or 776ins3-expressing oocyte. Note that the CBZ concentration was reduced for these two mutants. The ACh concentration of the test pulses was adjusted in both cases near their corresponding EC_{50} values. Bars and dashed lines, timing of the drug applications.

concluded that VPA does not interfere with these receptors. Indeed this VPA dose corresponds to ~10-fold the upper antiepileptic plasma level (antiepileptic range, 280–690 μ*M*), whereas VPA concentrations found in cerebrospinal fluid correspond to 10–15% of the plasma level (24). Given these results, VPA was not tested on $h\alpha_4(S248F)\beta_2$.

DISCUSSION

Although it is widely documented that most AEDs interact with voltage-dependent channels, much less is known about their possible interaction with other integral membrane proteins such as ligand-gated channels. Two exceptions are the benzodiazepines (BZDs) and barbiturates, which interact with the $GABA_A$ receptor. Electrophysiologic investigations done in neurons from the central nervous system (CNS) demonstrated that CBZ apparently enhances inactivation of sodium channels by shifting the inactivation curve toward more hyperpolarized voltages (1,25). Comparable findings were obtained by several laboratories on studies done on PHT (26–28), VPA (29–31), and LTG (32–34). However, in view of the specificity of CBZ versus VPA in partial epilepsies with frequent seizures (35,36) or in ADNFLE (14,15), it seems unlikely that the antiepileptic efficacy of CBZ can be attributed only to the interaction with sodium channels. It is therefore expected that CBZ might interact with other integral membrane proteins involved either in the signal transmission across neurons or in the regulation of the overall cell excitability.

Voltage-dependent potassium currents also were enhanced by low doses of CBZ in rat cortical neurons (37,38), whereas calcium currents were almost insensitive to CBZ (4). Several studies suggested that NMDA receptors are inhibited by CBZ. When applied to cortical wedges from epileptic mice, CBZ decreased the NMDA-induced depolarization (39). The increase of intracellular calcium concentration caused by NMDA activation in rat cerebellar granule cells was reduced by near-millimolar CBZ concentrations (8). In another study CBZ potentiated $GABA_A$ currents in cultured rat cortical neurons. The potentiation was dependent on the concentration of GABA, suggesting an allosteric modulation of the receptor, through a site distinct from BZD (6). CBZ also binds to adenosine receptors, but it is unlikely that this participates in its antiepileptic activity (40,41). Finally, an interaction of CBZ at antiepileptic concentrations with

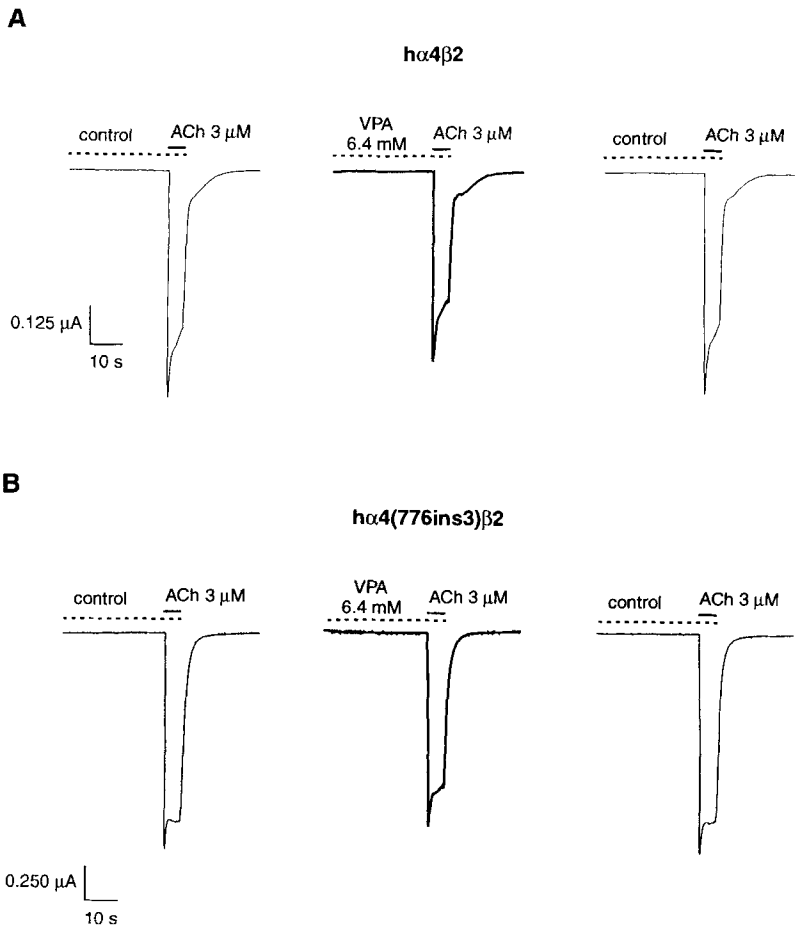

FIG. 5. Low sensitivity of $h\alpha_4\beta_2$ and an autosomal dominant nocturnal frontal lobe epilepsy (ADNFLE) mutant nicotinic acetylcholine receptor (nAChR) to valproate (VPA). **A, B:** Effects of pre- and coapplication of VPA (6.4 m*M*) on the ACh-evoked current for $h\alpha_4\beta_2$ and $h\alpha_4$(776ins3)β_2. Responses were recorded in the same cell before, during, and after VPA.

nicotinic receptors was suggested by Yoshimura et al. (7). They showed that CBZ inhibited carbachol-induced catecholamine secretion and calcium influx by inhibiting sodium influx through nAChRs in cultured bovine adrenal medullary cells.

The recent identification of a genetically transmissible form of epilepsy, ADNFLE (42), and its high sensitivity to CBZ (14–16), together with the discovery of a linkage to mutations within the α_4 subunit of the nAChRs (10, 11), reinforced the hypothesis of an effect of CBZ on nAChRs. The pentameric $\alpha_4\beta_2$ nAChR is the most abundant nAChR subtype found in vertebrate brain (43) and is widely distributed within the human CNS, with a particularly high density in the thalamus, the striatum, and the cortex (44). The two identified α_4 mutations yield an overall loss of function. Why a mutation in the widely distributed nAChRs causes a focal epilepsy in ADNFLE remains to be elucidated. A congenital abnormality of the nAChRs may have caused a modification of the establishment of appropriate neuronal connections, altering some CNS circuits, and eventually favoring epileptogenesis in frontal areas. The role of the nAChRs in the development of CNS has been suggested by (a) their very early expression in embryonic life, preceding innervation, and (b) the specific developmental patterns of their messenger RNA (mRNA) levels, temporally related to the timing of neuronal differentiation and establishment of connections (45–48). Another explanation could be the existence of a specific nAChR subunit distribution in different brain areas, with more receptors having incorporated mutant α_4 subunits in frontal lobes (15). The reduction in seizure frequency or the spontaneous remission of seizures with advancing age often observed in ADNFLE patients (14) may be related to the progressive spontaneous reduction of nAChRs with time. Indeed it was shown that nAChRs steadily decrease throughout life in the frontal lobe, whereas they remain approximately constant or increase in other areas (44). Thus a progressive reduction of deficient α_4 nAChRs may reduce the adverse effects provoked by the mutation. It can therefore be considered that either a compensatory mechanism takes place or that deficient nAChRs are more deleterious than missing receptors.

In this work we examined the effects of CBZ on the control and ADNFLE mutant human neuronal $\alpha_4\beta_2$ nAChRs reconstituted in *Xenopus* oocytes. Incubation of cells expressing the $h\alpha_4\beta_2$ nAChR in a solution containing CBZ in the 100 μM range resulted in a profound

reduction of the ACh-evoked current (IC_{50}, 140.5 μM). This inhibition was readily reversible by bathing the cell in control solution. The absence of modification of the IC_{50} in function of the ACh concentration indicates that CBZ acts as a noncompetitive blocker, whereas in a competitive inhibitor, blockade can be relieved by an increase of the agonist concentration. Two mechanisms may explain the observed CBZ blockade. On one hand, it can be proposed that CBZ acts as a negative allosteric effector, but on the other hand, it could be postulated that CBZ acts as an open channel blocker. A negative allosteric effector must fulfill the following criteria: (a) the inhibition of the ACh-evoked current should depend on the CBZ concentration and exposure duration but not on the channel opening, (b) dose–response inhibition curves should also depend on the ACh concentration, (c) a modification of the time course of the agonist-evoked current might be observed in presence of the effector [see (49)]. OCBs are often characterized by (a) a voltage dependence, (b) a time course of recovery that is influenced by the presence of agonist, and (c) a use-dependent mode of action. Furthermore, a rebound of the response at the end of the blockade is often observed as the antagonist leaves the channel while the agonist is still present in the receptors' vicinity.

Data presented illustrate that for the control $h\alpha_4\beta_2$ receptor, CBZ blockade occurs only when this compound is present at the same time as the agonist and that inhibition is independent of the ACh concentration. The increase in apparent desensitization rate observed in Fig. 2D must therefore be attributed to the progressive blockade of the receptor and not to an alteration of its intrinsic kinetic properties. The lack of voltage dependence can be attributed to the absence of charge on CBZ, which therefore cannot be influenced by the transmembrane potential. Finally, as seen in Fig. 4, the use-dependent blockade caused by a classic open channel blocker (MK-801) and CBZ displays comparable profiles. Taken together, these data suggest that CBZ acts on the control $h\alpha_4\beta_2$ as an open channel blocker and not as a negative allosteric effector.

Determination of the effects of CBZ on the two mutated nAChRs found in ADNFLE patients revealed an increase in the apparent sensitivity of these receptors. Both mutations are known to be in the second transmembrane domain that borders the wall of the ionic pore. Thus it might be expected, as shown for the muscle receptor (50), that these mutations could interact with a compound that binds within the channel lumen. Because it has been shown that a mutation in the second transmembrane domain can allosterically alter the receptor affinity to ACh (51), it could alternatively be considered that the increase of CBZ blockade arises from a different mechanism than that of the control receptor. Determination of CBZ mode of action on both the S248F and 776ins3 mutants confirmed that this compound acts only in presence of ACh and therefore must act as an OCB. The rebound observed at the end of each high concentration of antagonist application, as well as the use-dependent blockade, illustrates that CBZ must enter the ionic pore to exert its action. This deduction is further supported by the parallel increase in the apparent affinity to MK-801. It can therefore be proposed that the increase in CBZ apparent affinity results from the increase of CBZ binding in the channel and not from an allosteric effect.

Numerous compounds, such as the neuroleptic chlorpromazine, are already known to be OCBs on the muscle-type nAChRs (52). Some powerful neuronal $h\alpha_4\beta_2$ nAChR OCBs have been recently recognized: the classic NMDA antagonists amantadine and MK-801, as well as the calcium channel antagonist TMB-8 (23). CBZ is structurally related to MK-801 (Fig. 4). The IC_{50}s observed with CBZ on the mutant receptors were barely higher (42 and 51 μM) than those observed with the potent nAChR OCBs on $h\alpha_4\beta_2$ nAChR (3.5, 19, and 17.2 μM, respectively). It is interesting to note that in opposition to what we observed with CBZ and MK-801, Kuryatov et al. (13) showed that inhibition by amantadine was less potent on the S248F mutant receptor than on $h\alpha_4\beta_2$ nAChR. This difference can be explained by assuming that this compound blocks the channel at a slightly different level.

The observation of a linkage between ADNFLE and a mutation in the α_4 subunit of the neuronal nAChR implies that this receptor must play a role in triggering this particular form of genetically transmissible epilepsy (10,11). Therefore it can be proposed that the action of CBZ on neuronal nAChRs may be involved in its antiepileptic activity. Indeed relative IC_{50}s of the mutant nAChRs and the known antiepileptic plasma levels of CBZ (20–50 μM) as well as those expected for the CSF [5–15 μM, (9)] are in agreement. This is correlated with a greater effectiveness of CBZ in the ADNFLE syndrome than in other partial epilepsies. In agreement with this observation, the surprising lack of VPA efficacy on ADNFLE patients (14,15) correlates with the absence of action of this compound on the neuronal nAChR. Moreover, a clinical report indicated that in one patient, the cholinesterase inhibitor pyridostigmine was effective in reducing seizure frequency (15). Cholinesterase inhibitors have also been shown to block nicotinic responses, in rat striatal synaptosomes (44,53).

Based on the current knowledge of the nAChRs, different hypotheses for the pathophysiologic mechanisms of ADNFLE may be considered. Postsynaptic nAChRs, located in somatodendritic regions, cause a general depolarization of the neuron, whereas presynaptic receptors, located on synaptic boutons, and preterminal receptors, localized on terminal axonal branches (54), influ-

ence transmitter release. In the function of the cell on which nAChRs are located, physiologic ACh binding on presynaptic nAChRs can facilitate the release of different neurotransmitters, including GABA (54), glutamate (55–57), ACh, dopamine, or noradrenaline (44,58–60). In ADNFLE, defective presynaptic nAChRs could, during some stages of the sleep, prevent the increased release of GABA in some brain areas and provoke an imbalance between excitation and inhibition.

Another hypothesis for the pathogenesis of ADNFLE is the alteration of the postsynaptic nAChRs in the pathways responsible for spindle generation and arousals. It is known that ADNFLE seizures occur mainly during stage 2 of non–rapid eye movement (REM) sleep (61), characterized by the highest rate of spindle activity. The change in EEG pattern from the synchronized (sleep) to the desynchronized (waking) state is essentially attributable to two components: a brainstem–thalamic cholinergic effect disrupting spindle oscillations and a concerted action exerted on the cerebral cortex by cholinergic basal forebrain neurons and by glutamatergic thalamocortical neurons (62). Nicotinic receptors have been identified on the thalamocortical cells that receive the cholinergic input from the tegmentum. It was shown in the rat that these receptors probably result from the assembly of the α_4 and β_2 subunits (63). In the cat, the activation of the cholinergic input of the thalamus was shown to disrupt spindle activity by an initial fast membrane depolarization of thalamocortical neurons, mediated by nicotinic receptors, followed by a prolonged depolarization mediated by muscarinic receptors (62). A nicotinic activation of the reticular thalamic nucleus/perigeniculate nucleus also may contribute to the cessation of spindles (64). In contrast, cholinergic basal forebrain projections to the neocortex activate muscarinic receptors (65). Thus it can be postulated that in ADNFLE, at the time of an arousal from sleep stage 2, the deleterious function of the nAChRs may prevent cessation of the synchronous activity in the thalamus, whereas an immediate arousal is induced in the neocortex. The temporary mismatch between the "level of vigilance" in the thalamus and the cortex could lead to abnormal activity in a thalamofrontal loop. A similar hypothesis of inequality between the basal and mesencephalic cholinergic thalamocortical inputs was recently proposed in absence epilepsy in rats by Danober et al. (66).

It is still difficult to propose a conclusive hypothesis that would explain why inhibition of the nAChRs by CBZ can be beneficial in ADNFLE patients. Because the $\alpha_4\beta_2$ nAChR is already hypoactive in these patients, the further inhibition by CBZ is rather surprising. However, suppression of a defective receptor may be less deleterious than its functioning. This might correlate with the age-related favorable outcome of ADNFLE and reduction in nAChRs density in the frontal cortex with age.

In conclusion, this work illustrates that the genetic polymorphisms of integral membrane proteins, such as those of a ligand-gated channel in ADNFLE patients, can result in a difference of sensitivity to drugs in clinical use. This may explain the individual specific sensitivity or insensitivity to a given compound.

Acknowledgment: We thank Drs S. Berkovic, A. Magnusson, and S. Weiland for their kind contribution and pleasant collaboration and Prof. C. Marescaux for continual discussion and helpful suggestions. This work was supported by the Swiss National Foundation no. 31-37191.93, the "Office Fédéral de l'Education et des Sciences," and the Swiss Priority Program (PNR38) 4038-044050 to D.B. Work done in O.K.S. laboratory was supported by a grant by the Deutsche Forschungsgemeinschaft (SFB 400/B5).

REFERENCES

1. Willow M, Gonoi T, Catterall WA. Voltage clamp analysis of the inhibitory actions of diphenylhydantoin and carbamazepine on voltage-sensitive sodium channels in neuroblastoma cells. *Mol Pharmacol* 1985;27:549–58.
2. McLean MJ, Macdonald RL. Carbamazepine and 10,11-epoxycarbamazepine produce use- and voltage-dependent limitation of rapidly firing action potentials of mouse central neurons in cell culture. *J Pharmacol Exp Ther* 1986;238:727–38.
3. Schwarz JR, Grigat G. Phenytoin and carbamazepine: potential- and frequency-dependent block of Na currents in mammalian myelinated nerve fibers. *Epilepsia* 1989;30:286–94.
4. Sayer RJ, Brown AM, Schwindt PC, Crill WE. Calcium currents in acutely isolated human neocortical neurons. *J Neurophysiol* 1993; 69:1596–606.
5. Kito M, Maehara M, Watanabe K. Antiepileptic drugs: calcium current interaction in cultured human neuroblastoma cells. *Seizure* 1994;3:141–9.
6. Granger P, Biton B, Faure C, et al. Modulation of the γ-aminobutyric acid type A receptor by the antiepileptic drugs carbamazepine and phenytoin. *Mol Pharmacol* 1995;47:1189–96.
7. Yoshimura R, Yanagihara N, Terao T, Minami K, Abe K, Izumi F. Inhibition by carbamazepine of various ion channels-mediated catecholamine secretion in cultured bovine adrenal medullary cells. *Naunyn Schmiedebergs Arch Pharmacol* 1995;352:297–303.
8. Hough CJ, Irwin RP, Gao X-M, Rogawski MA, Chuang D-M. Carbamazepine inhibition of *N*-methyl-D-aspartate-evoked calcium influx in rat cerebellar granule cells. *J Pharmacol Exp Ther* 1996; 276:143–9.
9. Morselli PL. Carbamazepine: absorption, distribution, and excretion. In: Levy RH, Mattson RH, Meldrum BS, eds. *Antiepileptic drugs*. New York: Raven Press, 1995:515–28.
10. Steinlein OK, Mulley JC, Propping P, et al. A missense mutation in the neuronal nicotinic acetylcholine receptor alpha 4 subunit is associated with autosomal dominant nocturnal frontal lobe epilepsy. *Nature Genet* 1995;11:201–3.
11. Steinlein OK, Magnusson A, Stoodt J, et al. An insertion mutation of the CHRNA4 gene in a family with autosomal dominant nocturnal frontal lobe epilepsy. *Hum Mol Genet* 1997;6:943–7.
12. Weiland S, Witzemann V, Villarroel A, Propping P, Steinlein O. An amino acid exchange in the second transmembrane segment of a neuronal nicotinic receptor causes partial epilepsy by altering its desensitization kinetics. *FEBS Lett* 1996;398:91–6.
13. Kuryatov A, Gerzanich V, Nelson M, Olale F, Lindstrom J. Mutation causing autosomal dominant nocturnal frontal lobe epilepsy alters Ca^{2+} permeability, conductance, and gating of human $\alpha_4\beta_2$ nicotinic acetylcholine receptors. *J Neurosci* 1997;17:9035–47.
14. Scheffer IE, Bhatia KP, Lopes-Cendes I, et al. Autosomal dominant nocturnal frontal lobe epilepsy: a distinctive clinical disorder. *Brain* 1995;118:61–73.
15. Hayman M, Scheffer IE, Chinvarun Y, Berlangieri SU, Berkovic

SF. Autosomal dominant nocturnal frontal lobe epilepsy: demonstration of focal frontal onset and intrafamilial variation. *Neurology* 1997;49:969–75.

16. Picard F, Rudolf G, Sebastianelli R, et al. A clinical study of 21 European families with dominant partial epilepsy. In: Berkovic S, Genton P, Hirsch E, Picard F, eds. *Genetics of focal epilepsies.* London: John Libbey, 1999:115–21.
17. Bertrand D, Cooper E, Valera S, Rungger D, Ballivet M. Electrophysiology of neuronal nicotinic acetylcholine receptors expressed in *Xenopus* oocytes following nuclear injection of genes or cDNA. In: Conn M, ed. *Methods in neuroscience.* New York: Academic Press, 1991:174–93.
18. Buisson B, Gopalakrishnan M, Arneric SP, Sullivan JP, Bertrand D. Human $\alpha_4\beta_2$ neuronal nicotinic acetylcholine receptor in HEK-293 cells: a patch-clamp study. *J Neurosci* 1996;16:7880–91.
19. Faigle JW, Feldmann KF. Carbamazepine: chemistry and biotransformation. In: Levy RH, Mattson RH, Meldrum BS, eds. *Antiepileptic drugs.* New York: Raven Press, 1995:499–513.
20. Ogden DC, Siegelbaum SA, Colquhoun D. Block of acetylcholine-activated ion channels by an uncharged local anaesthetic. *Nature* 1981;289:596–8.
21. Bertrand S, Weiland S, Berkovic SF, Steinlein OK, Bertrand D. Properties of neuronal nicotinic acetylcholine receptor mutants from humans suffering from autosomal dominant nocturnal frontal lobe epilepsy. *Br J Pharmacol* 1998;125:751–60.
22. Buisson B, Curtis L, Bertrand D. Neuronal nicotinic acetylcholine receptor and epilepsy. In: Berkovic S, Genton P, Hirsch E, Picard F, eds. *Genetics of focal epilepsies.* London: John Libbey, 1999: 187–202.
23. Buisson B, Bertrand D. Open-channel blockers at the human $\alpha_4\beta_2$ neuronal nicotinic acetylcholine receptor. *Mol Pharmacol* 1998; 53:555–63.
24. Levy RH, Shen DD. Valproic acid: absorption, distribution, and excretion. In: Levy RH, Mattson RH, Meldrum BS, eds. *Antiepileptic drugs.* New York: Raven Press, 1995:605–19.
25. Kuo CC, Chen RS, Lu L, Chen RC. Carbamazepine inhibition of neuronal Na^+ currents: quantitative distinction from phenytoin and possible therapeutic implications. *Mol Pharmacol* 1997;51:1077–83.
26. Matsuki N, Quandt FN, Ten Eick RE, Yeh JZ. Characterization of the block of sodium channels by phenytoin in mouse neuroblastoma cells. *J Pharmacol Exp Ther* 1984;228:523–30.
27. Tomaselli GF, Marban E, Yellen G. Sodium channels from human brain RNA expressed in *Xenopus* oocytes: basic electrophysiologic characteristics and their modification by diphenylhydantoin. *J Clin Invest* 1989;83:1724–32.
28. Wakamori M, Kaneda M, Oyama Y, Akaike N. Effects of chlordiazepoxide, chlorpromazine, diazepam, diphenylhydantoin, flunitrazepam and haloperidol on the voltage-dependent sodium current of isolated mammalian brain neurons. *Brain Res* 1989;494:374–8.
29. Van den Berg RJ, Kok P, Voskuyl RA. Valproate and sodium currents in cultured hippocampal neurons. *Exp Brain Res* 1993;93: 279–87.
30. Taverna S, Mantegazza M, Franceschetti S, Avanzini G. Valproate selectively reduces the persistent fraction of Na^+ current in neocortical neurons. *Epilepsy Res* 1998;32:304–8.
31. Vreugdenhil M, van Veelen CW, van Rijen PC, Lopes da Silva FH, Wadman WJ. Effect of valproic acid on sodium currents in cortical neurons from patients with pharmaco-resistant temporal lobe epilepsy. *Epilepsy Res* 1998;32:309–20.
32. Mutoh K, Dichter MA. Lamotrigine blocks voltage-dependent Na currents in a voltage-dependent manner with a small use-dependent component. *Epilepsia* 1993;34:87.
33. Macdonald RL, Kelly KM. Antiepileptic drug mechanisms of action. *Epilepsia* 1995;36:S2–12.
34. Kuo CC. A common anticonvulsant binding site for phenytoin, carbamazepine, and lamotrigine in neuronal Na^+ channels. *Mol Pharmacol* 1998;54:712–21.
35. Mattson RH, Cramer JA, Collins JF. A comparison of valproate with carbamazepine for the treatment of complex partial seizures and secondarily generalized tonic-clonic seizures in adults. *N Engl J Med* 1992;327:765–71.
36. Seino M. A comment on the efficacy of valproate in the treatment of partial seizures. *Epilepsia* 1994;35:S101–4.
37. Zona C, Tancredi V, Palma E, Pirrone GC, Avoli M. Potassium currents in rat cortical neurons in culture are enhanced by the antiepileptic drug carbamazepine. *Can J Physiol Pharmacol* 1990; 68:545–7.
38. Olpe H, Kolb CN, Hausdorf A, Haas HL. 4-Aminopyridine and barium chloride attenuate the anti-epileptic effect of carbamazepine in hippocampal slices. *Experientia* 1991;47:254–7.
39. Lancaster JM, Davies JA. Carbamazepine inhibits NMDA-induced depolarizations in cortical wedges prepared from DBA/2 mice. *Experientia* 1992;48:751–3.
40. Clark M, Post RM. Carbamazepine, but not caffeine, is highly selective for adenosine A1 binding sites. *Eur J Pharmacol* 1989; 164:399–401.
41. Okada M, Kiryu K, Kawata Y, et al. Determination of the effects of caffeine and carbamazepine on striatal dopamine release by in vivo microdialysis. *Eur J Pharmacol* 1997;321:181–8.
42. Phillips HA, Scheffer IE, Berkovic SF, Hollway GE, Sutherland GR, Mulley JC. Localization of a gene for autosomal dominant nocturnal frontal lobe epilepsy to chromosome 20q13.2. *Nat Genet* 1995;10:117–8.
43. Whiting PJ, Lindstrom JM. Characterization of bovine and human neuronal nicotinic acetylcholine receptors using monoclonal antibodies. *J Neurosci* 1988;8:3395–404.
44. Gotti C, Fornasari D, Clementi F. Human neuronal nicotinic receptors. *Prog Neurobiol* 1997;53:199–237.
45. Court J, Clementi F. Distribution of nicotinic subtypes in human brain. *Alzheimer Dis Assoc Disord* 1995;9:6–14.
46. Zoli M, Le Novère N, Hill JAJ, Changeux J-P. Developmental regulation of nicotinic ACh receptor subunit mRNAs in the rat central and peripheral nervous systems. *J Neurosci* 1995;15:1912–39.
47. Schröder H, Wevers A, Happich E, Schütz U, Moser N. Molecular histochemistry of nicotinic receptors in human brain. In: Becker R, Giacobini E, eds. *Alzheimer disease: from molecular biology to therapy.* Boston: Birkhäuser, 1996:269–73.
48. Agulhon C, Charnay Y, Vallet P, Bertrand D, Malafosse A. Distribution of mRNA for the α_4 subunit of the nicotinic acetylcholine receptor in the human fetal brain. *Brain Res Mol Brain Res* 1998; 58:123–31.
49. Rubin MM, Changeux JP. On the nature of allosteric transitions; implications of nonexclusive ligand binding. *J Mol Biol* 1966;21: 265–74.
50. Leonard RJ, Labarca CG, Charnet P, Davidson N, Lester HA. Evidence that the M2 membrane-spanning region lines the ion channel pore of the nicotinic receptor. *Science* 1988;242:1578–81.
51. Bertrand D, Changeux JP. Nicotinic receptor: an allosteric protein specialized for intercellular communication. *Semin Neurosci* 1995; 7:75–90.
52. Arias HR. Luminal and non-luminal non-competitive inhibitor binding sites on the nicotinic acetylcholine receptor [Review]. *Mol Membr Biol* 1996;13:1–17.
53. Clarke PB, Reuben M, el-Bizri H. Blockade of nicotinic responses by physostigmine, tacrine and other cholinesterase inhibitors in rat striatum. *Br J Pharmacol* 1994;111:695–702.
54. Léna C, Changeux J-P, Mulle C. Evidence for "preterminal" nicotinic receptors on GABAergic axons in the rat interpeduncular nucleus. *J Neurosci* 1993;13:2680–8.
55. Vidal C, Changeux JP. Nicotinic and muscarinic modulations of excitatory synaptic transmission in the rat prefrontal cortex in vitro. *Neuroscience* 1993;56:23–32.
56. McGehee DS, Heath MJS, Gelber S, Devay P, Role LW. Nicotine enhancement of fast excitatory synaptic transmission in CNS by presynaptic receptors. *Science* 1995;269:1692–6.
57. Gray R, Rajan AS, Radcliffe KA, Yakehiro M, Dani JA. Hippocampal synaptic transmission enhanced by low concentrations of nicotine. *Nature* 1996;383:713–6.

58. Marshall DL, Redfern PH, Wonnacott S. Presynaptic nicotinic modulation of dopamine release in the three ascending pathways studied by in vivo microdialysis: comparison of naive and chronic nicotine-treated rats. *J Neurochem* 1997;68:1511–9.
59. Wonnacott S. Presynaptic nicotinic ACh receptors. *Trends Neurosci* 1997;20:92–8.
60. Li X, Rainnie DG, McCarley RW, Greene RW. Presynaptic nicotinic receptors facilitate monoaminergic transmission. *J Neurosci* 1998;18:1904–12.
61. Oldani A, Zucconi M, Ferini-Strambi L, Bizzozero D, Smirne S. Autosomal dominant nocturnal frontal lobe epilepsy: electroclinical picture. *Epilepsia* 1996;37:964–76.
62. Curró Dossi R, Paré D, Steriade M. Short-lasting nicotinic and long-lasting muscarinic depolarizing responses of thalamocortical neurons to stimulation of mesopontine cholinergic nuclei. *J Neurophysiol* 1991;65:393–406.
63. Lavine N, Reuben M, Clarke PBS. A population of nicotinic receptors is associated with thalamocortical afferents in the adult rat: laminal and areal analysis. *J Comp Neurol* 1997;380:175–90.
64. Lee KH, McCormick DA. Acetylcholine excites GABAergic neurons of the ferret perigeniculate nucleus through nicotinic receptors. *J Neurophysiol* 1995;73:2123–8.
65. Mesulam M-M. The systems-level organization of cholinergic innervation in the human cerebral cortex and its alterations in Alzheimer's disease. *Prog Brain Res* 1996;109:285–97.
66. Danober L, Deransart C, Depaulis A, Vergnes M, Marescaux C. Pathophysiological mechanisms of genetic absence epilepsy in the rat. *Prog Neurobiol* 1998;55:27–57.